*Desalination and Water Treatment*
www.deswater.com

doi: 10.1080/19443994.2016.1141376

57 (2016) 24267–24277
November

Taylor & Francis
Taylor & Francis Group

# The effect of functionalized MWCNT and SDS on the characteristic and performance of PAN ultrafiltration membrane

Zahra Dastbaz[a], Majid Pakizeh[a,*], Mahdieh Namvar-Mahboub[b]

[a]*Faculty of Engineering, Department of Chemical Engineering, Ferdowsi University of Mashhad, P.O. Box 9177948974, Mashhad, Iran, Tel. +98 51 57260740; email: z.dastbaz@gmail.com (Z. Dastbaz), Tel./Fax: +98 5138816840; email: pakizeh@um.ac.ir (M. Pakizeh)*

[b]*Department of Chemical Engineering, University of Gonabad, Gonabad, Iran, Tel. +9851 57260740; email: namvarmahboob@yahoo.com*

Received 4 October 2015; Accepted 8 January 2016

ABSTRACT

In this study, the influence of functionalized multi-walled carbon nanotube (F-MWCNT), sodium dodecyl sulfate (SDS) on the characteristic and performance of polyacrylonitrile (PAN) membrane was studied. The mixed matrix membranes were prepared via solution blending and phase inversion methods. MWCNTs were acidified and then functionalized by amino group using microwave. Three dosage of F-MWCNT, i.e. 0.5, 1 and 2 wt.%, and two dosage of SDS, i.e. 2.5 and 5 wt.%, were used to prepare mixed matrix membranes. The as-prepared membranes were characterized by scanning electron microscopy (SEM), field emission scanning electron microscopy (FESEM), atomic force microscopy (AFM), contact angle, and Fourier transform infrared spectroscopy. The hydrophilicity and pure water flux increased with addition of both additives. Separation performance of Bovine serum albumin (BSA) was investigated in three different pHs (5, 7 and 9). The results showed that both additives enhanced performance parameters of pure PAN membrane. From the results it is found that 0.5 wt.% of F-MWCNT and 2.5 wt.% of SDS, are the optimum values to achieve maximum permeate flux and BSA rejection, respectively.

*Keywords:* Polyacrylonitrile; SDS surfactant; Ultrafiltration membrane; Functionalized carbon nanotube; Hydrophilicity

## 1. Introduction

In the recent decades, ultrafiltration membrane technology has gained importance to solve a lot of separation problems in different industries [1,2]. One of the restrictions which ultrafiltration polymeric membranes encounter is fouling. Fouling declines the permeate flux and rejection of membrane over a period of operation as a result of the undesirable adsorption of solute onto the surface or into pores of membrane [2–4]. Surface morphology and physico-chemical properties of membrane affect their fouling resistance characteristic [5]. Generally, hydrophilic membranes are more resistant to fouling, but they show poor mechanical and chemical stability. One of the commercial membranes which commonly used for ultrafiltration process is polyacrylonitrile (PAN) membranes. PAN membrane depicts relatively hydrophilic chemistry with appropriate stability to hydrolysis and

*Corresponding author.

oxidation. Nevertheless, the PAN UF membranes still suffer from significant fouling [6,7]. In this case, modification of the membrane material and morphology seems to be essential.

One approach to improve properties of polymeric (especially PAN) membrane is the use of bulk modification technique. In this method, polymer is blended with one or more additives as modified materials to prepare casting solution [8]. Among the various additives which can be applied as modifier, MWCNTs have attracted a lot of consideration because of their extraordinary properties such as high special surface area, easy functionalization, chemical stability, mechanical strength, and thermal conductance [9,10]. However, they have been surrounded by some problems like their tendency to aggregate in polymer matrix and absence of interfacial holding due to their molecularly smooth surface. Hence, homogeneous scattering and solid interfacial collaboration are key issues in augmenting the preference of CNTs fortification [10]. Besides, surfactants constitute the most important group of detergents which are generally used to improve hydrophilicity and structure of UF membranes owing to their special structure (composed of a hydrophobic tail which attached to a hydrophilic head) [11].

There are some researches which have been developed to change the surface properties of PAN membrane using bulk modification method. Zhi et al. [12] used poly (N,N-dimethylaminoethyl methacrylate)-grafted silica nanoparticles as hydrophilic additives to modify PAN membrane. They observed that composite membrane had higher porosity, pure water flux and BSA rejection than pure PAN membrane. This result was attributed to increasing hydrophilicity of composite membrane. Majeed et al. [13] modified PAN ultrafiltration membrane by incorporation of oxidized-MWCNTs (O-MWCNTs) into polymer matrix and observed that the hydrophilicity and pure water flux increased by adding O-MWCNTs. Su et al. [14] stated that grafting PEG to PAN led to formation of membrane with hydrophilic properties and increased its antifouling capability. Yang and Liu [15] illustrated that using $CaCl_2$ as an additive in PAN ultrafiltration membrane enhanced its permeability. Shekarian et al. [16] added IGEPAL as surfactant to PAN polymeric membrane. The surface morphology and hydrophilic properties of prepared membrane was evaluated using scanning electron microscopy (SEM) and contact angle (CA) measurement. Their results showed that addition of surfactant increased water flux and decreased protein rejection percentage.

To the best of author's knowledge, the modification of PAN UF membrane using amine-functionalized MWCNT or sodium dodecyl sulfate (SDS) as additives is not investigated previously.

In this study, mixed matrix UF membranes including nanomaterials and/or surfactant as additive were prepared, characterized and used in BSA recovery. MWCNT were acidified and then modified by ethylene diamine (EDA) to ensure appropriate adhesion between polymer chains and functionalized multi-walled carbon nanotube (F-MWCNT). Fourier transform infrared spectroscopy (FTIR) was performed to characterize F-MWCNT. To modify the PAN membrane, the F-MWCNT, and SDS were used as nanomaterials and surfactant, respectively. The as-prepared UF membranes were characterized using SEM, field emission scanning electron microscopy (FESEM), atomic force microscopy (AFM), FTIR, and CA tests. Beside, the rejection of BSA and permeate flux of mixed matrix membranes were investigated.

## 2. Material and methods

### 2.1. Materials

PAN ($M_W$ = 150,000 g/mol), nitric acid ($HNO_3$), sodium hydroxide (NaOH), Methanol ($CH_3OH$) and hydrochloric acid (HCl) was supplied by Sigma-Aldrich. N,N-dimethylformamide (DMF), SDS ($M_W$ = 288,000 g/mol), and sulfuric acid ($H_2SO_4$) was purchased from Merck. MWCNTs (95% purity) with an average length of 30 μm and 10–20 nm in outer diameter were provided by Shenzhen Nano-Tech Port Company. EDA from Guangdong Guanghua chemical factory was used as functionalizing agent. Bovine serum albumin (BSA) was purchased from Pan Reac Applichem ITW reagent (Germany). PTFE membranes (pore size of 0.2 μm) were obtained from Whatman Company.

### 2.2. Preparation of functionalized MWCNTs

At first, in order to treat MWCNTs, 1 g of raw MWCNTs was added to 80 mL of mixture of $H_2SO_4$/$HNO_3$ (3:1 in vol. %) and heated at 70˚C for 8 h without stirring. Then solution was diluted with 1 L of deionized water and filtered through a PTFE membrane. The oxidized MWCNTs were rinsed with deionized water. After that, O-MWCNTs were dried in an oven at 60˚C for 24 h. The resulted O-MWCNTs were functionalized with amine groups according to the protocol presented by Amiri et al. [17]. Briefly, 0.2 g of the O-MWCNTs was sonicated with 20 mL of EDA for 30 min at 50˚C. Then the prepared suspension was poured into a teflon reaction vessel, placed in microwave chamber (LG-4284TCR) and was heated in microwave up to 90˚C for 15 min with output power of 500 W. Afterward, the resulted suspension

was cooled to room temperature, and filtered through a PTFE membrane. Finally, F-MWCNT were washed more than seven times with DMF and methanol to remove any un-reacted EDA and then dried for 48 h at 50˚C.

### 2.3. Preparation of mixed matrix membrane

PAN/F-MWCNTs, PAN/SDS, and PAN/F-MWCNTs/SDS mixed matrix membranes were prepared by phase inversion method. To use the first additive, different dosage (0–2 wt.%) of the F-MWCNTs was dissolved in DMF and sonicated for at least 30 min to form proper dispersion of nanoparticles. Then PAN was gradually added into dispersed solution of MWCNTs to get 15 wt.% of polymer in dope solution. The dope solution was mixed at 70˚C with magnetic stirrer at 200 rpm for 30 h. After degassing at room temperature, the solution was cast on glass plate using adjustable casting bar (NEU-TEK22812059, Spain) with 200 μm thickness. Finally, the casted film immersed in the water bath for at least 24 h.

To prepare PAN/SDS membrane, different dosage (2.5 and 5%) of SDS was added to PAN/DMF solution of 15 wt.%, and then stirred at 70˚C with magnetic stirrer at 200 rpm for 48 h. Then the solution was casted on glass plate and immersed in water bath to prepare PAN/SDS membrane. All the as-prepared membranes were nominated based on the additive dosage in the casting solution (Table 1).

### 2.4. Membrane characterization

#### 2.4.1. FTIR spectroscopy

The FTIR spectra were applied to investigate the grafted groups onto the surface of F-MWCNTs. Results for pristine, acidified and amine-functionalized MWCNTs were obtained using FTIR Avater 370 Nicolet Spectrometer.

#### 2.4.2. SEM and FESEM analysis

The morphologies of pure PAN and modified membranes were observed by scanning electron microscope (SEM, LEO1450VP, Zeiss, Germany) at 20 kV. Membranes were fractured in liquid nitrogen to obtain clean cut for cross sectional view. All samples were sputtered with a thin layer of gold-palladium using SC7620 (Quorum Technologies England) prior to analysis. Besides, the presence of F-MWCNTs on the surface of modified membrane was directly observed by FESEM (ZIGMA/VP, Zeiss, Germany).

#### 2.4.3. Atomic force microscopy

Surface roughness of pure and PAN/F-MWCNTs membranes was acquired using AFM (Easyscan2 Flex AFM, Switzerland). All analysis were conducted at scan size of $10 \times 10$ μm and roughness parameter of fabricated membranes including the average arithmetic roughness ($R_a$), root mean square ($R_q$), and the mean difference between the highest and lowest areas ($R_z$) was evaluated.

#### 2.4.4. CA measurements

To determine the hydrophilicity of fabricated membranes, the CA of membranes were measured by CA measuring instrument (OCA15 plus, 196Data physics, Germany). Deionized water was utilized as the test fluid for the estimations. The reported results are the average CA of three measurements on each sample.

#### 2.4.5. Water flux and membrane separation

A cross flow membrane setup with a membrane effective area of 9.61 $cm^2$ was used to determine pure water flux and BSA rejection. Ultrafiltration test was evaluated under condition of 25˚C and 0.2 MPa with deionized water. Permeate flux was calculated as follows (Eq. (1)):

Table 1
Composition of casting solution for prepared membranes

| Membrane code | PAN (wt.%) | F-MWCNTs (wt.%) | SDS (wt.%) | DMF (wt.%) |
|---|---|---|---|---|
| PAN0 | 15 | 0 | 0 | 85 |
| PAN-C0.5 | 15 | 0.5 | 0 | 84.5 |
| PAN-C1 | 15 | 1 | 0 | 84 |
| PAN-C2 | 15 | 2 | 0 | 83 |
| PAN-S2.5 | 15 | 0 | 2.5 | 82.5 |
| PAN-S5 | 15 | 0 | 5 | 80 |

$$J_{w1} = \frac{V}{A \cdot \Delta t} \quad (1)$$

where $J_{w1}$ represents flux of membranes (L/(m$^2$ h)), $V$ is the permeate volume (L), $A$ is membranes effective surface area (m$^2$), and $\Delta t$ is the time (h).

BSA solution as a feed and fouling agent was selected for investigating performance of as-prepared membranes. The concentration of BSA in feed solution was set to 1 mol/L. The feed was prepared in three pH, i.e. 5, 7, and 9, using HCl and NaOH solutions (2 M) and was measured by a pH meter apparatus (HANNA Instruments). Feed and permeate concentration $C_f$ and $C_p$, respectively, was measured by UV-2100 spectrophotometer and BSA rejection ($R$) was calculated according to Eq. (2):

$$R\,(\%) = \left(1 - \frac{C_p}{C_f}\right) \times 100 \quad (2)$$

## 3. Results and discussion

### 3.1. Characterization of F-MWCNTs

The FTIR spectra of pristine, acidic, and amine-functionalized MWCNTs are shown in Fig. 1. The FTIR spectra of pristine MWCNTs shows the characteristic band at 1,515 cm$^{-1}$ which is attributed to C=C bond. This result proves the presence of carbon at the pristine MWCNT [18,19]. For oxidized MWCNT, the bands at 1,708 and 3,418 cm$^{-1}$ are corresponded to COOH and OH functional groups after acidification of MWCNTs [9,18]. These bounds reveal that raw MWCNT is successfully oxidized by concentrated acid mixture. Moreover, the FTIR spectra of F-MWCNT shows change when compared with FTIR spectra of raw and oxidized MWCNT. The band at 1,553 cm$^{-1}$ is corresponded to bending of $NH_2$ bond on the surface of amine-functionalized MWCNTs. At 3,448 cm$^{-1}$ OH group overlapped $NH_2$ stretching bond of amine group [9,18]. New bond at 1,624 cm$^{-1}$ attributed to C=O groups overlapped with C=C band [16]. The results indicate that amine functional groups are located on the surface of MWCNTs after functionalization.

### 3.2. Characterization of mixed matrix membranes

#### 3.2.1. Membrane morphology

Fig. 2 shows surface morphology of mixed matrix membranes with different filler dosage. As illustrated in Fig. 2(a)–(d), the surface morphology of PAN/F-MWCNT membranes has drastically been changed when compared with the surface of pure PAN membrane. In this case, the pore-like structure on the surface of pure PAN membrane has disappeared by incorporating F-MWCNT into polymer matrix. When F-MWCNT nanoparticles are added to polymer solution, they increase the viscosity of casting solution. Therefore, the void formation on surface of prepared membrane is suppressed due to delayed demixing [20,21]. The F-MWCNT may also block the pores attributed to their hindrance effect. Nevertheless, the presence of hydrophilic F-MWCNT particles accelerates DMF-water exchange and as a consequence the instantaneous demixing may occur. In this case, it seems that the effect of filler on solution viscosity overcome its effect on solvent-nonsolvent exchange rate during phase inversion process.

The SEM images of PAN/SDS membrane surface are presented in Fig. 2(e)–(f). As can be seen, for membrane with 2.5 wt.% of SDS in the casting solution, the top surface become denser when compared with that one of pure PAN membrane. Further

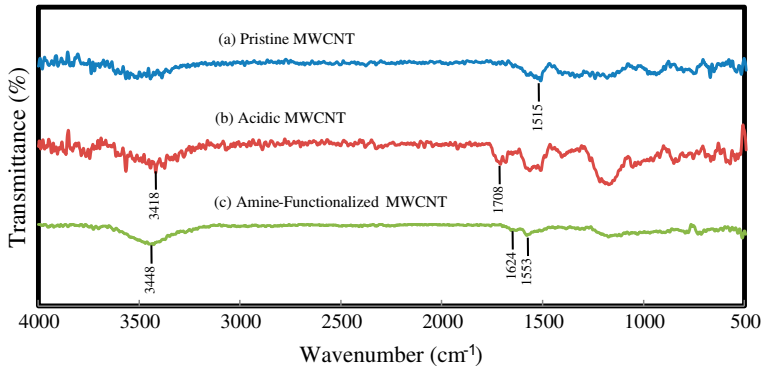


Fig. 1. FTIR spectra of (a) pristine MWCNT, (b) Acidic MWCNT, and (c) Amine-functionalized MWCNT.

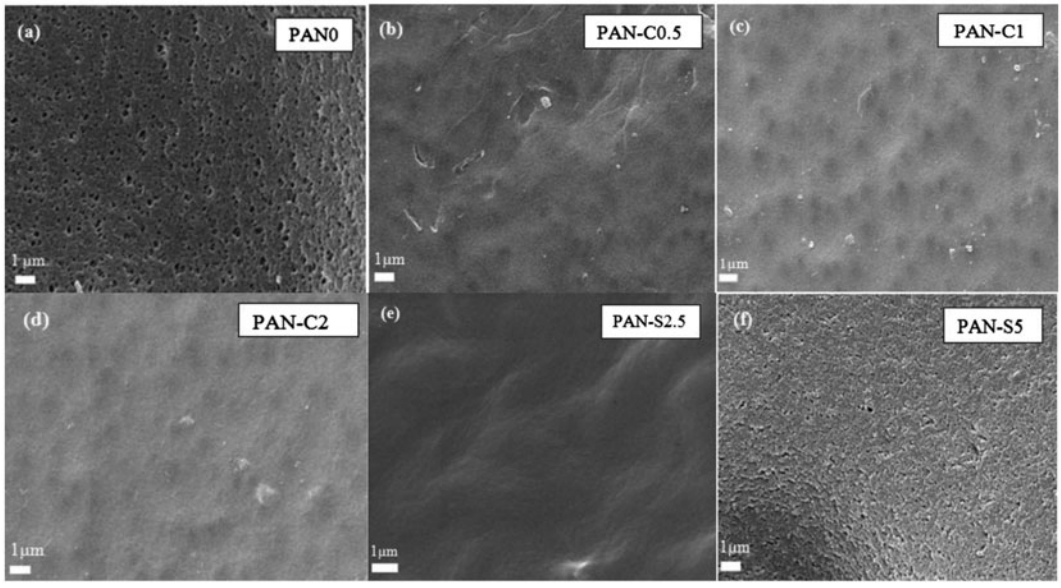


Fig. 2. Surface morphology of (a) PAN0, (b) PAN-C0.5, (c) PAN-C1, (d) PAN-C2, (e) PAN-S2.5, and (f) PAN-S5.

increase in SDS dosage to 5 wt.% promotes the formation of pores on the membrane surface. Since critical micelle concentration of SDS is lower than SDS dosage, micelles could form with non-polar group outside and polar group inside the micelles. These free micelles drive out from the top layer of membrane during solvent–nonsolvent exchange and consequently leave voids in the membrane surface [22]. However, it seems that pore size of surface of PAN-S5 is fairly lower than that one of PAN membrane due to higher viscosity of PAN/SDS solution in comparison with pure PAN solution.

The FESEM images of surface morphology of pure PAN and PAN-C2 membranes are presented in Fig. 3. From this figure, it can be found that F-MWCNTs are presented on the surface of PAN-C2 mixed matrix membrane. Besides, as illustrated in Fig. 3, there is no defect in polymer-MWCNT interface due to proper compatibility between the F-MWCNTs and polymer chains. Indeed, the interaction between $NH_2$ group of F-MWCNT surface and nitrile group of PAN matrix causes an appropriate PAN-F-MWCNT adhesion [23]. It has also observed that MWCNTs are well dispersed into polymer matrix.

The cross-sectional morphology of the pure PAN and modified membranes are shown in Fig. 4. Cross-sectional view of as-prepared membranes demonstrate asymmetric structure including skin top layer and finger-like sublayer. This structure is a result of rapid exchange between DMF as solvent and water as non-solvent in phase inversion process [18]. According to Fig. 4(a)–(d), the size of macrovoids of sublayer have been changed and finger-like cavities were fully developed through sublayer with increasing MWCNTs dosage from 0 to 2%. Indeed, the presence of hydrophilic F-MWCNTs in PAN matrix accelrates

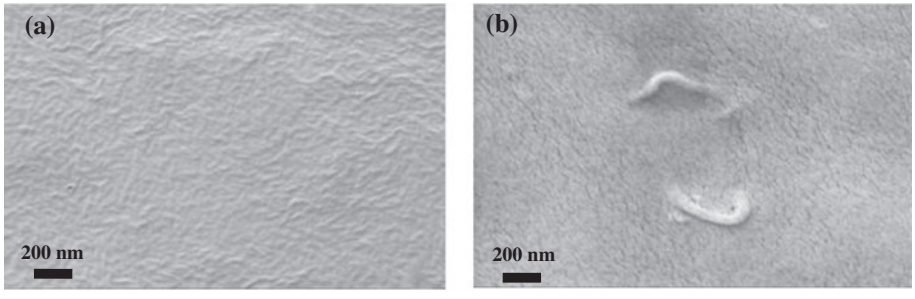


Fig. 3. FESEM images of surface of (a) PAN0 and (b) PAN-C2.

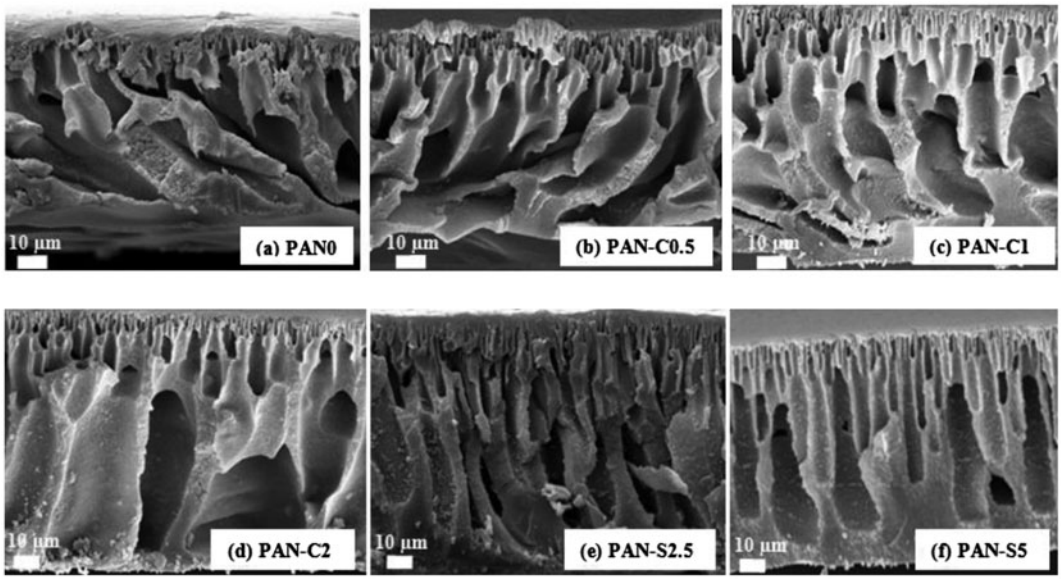


Fig. 4. Cross-sectional view of (a) PAN0, (b) PAN-C0.5, (c) PAN-C1, (d) PAN-C2, (e) PAN-S2.5, and (f) PAN-S5.

solvent-nonsolvent exchange which promotes instantanous demixing during immersion of film in coagulation bath. It seems that this is dominant factor which affect morphologty of sublayer. The same influence of addition of MWCNTs into polymer matrix were observed by Celik et al. [24].

Also, Fig. 4(e)–(f) shows PAN membrane blended with SDS in 2.5 and 5 wt.%. The SEM images depict that the addition of SDS as a hydrophilic additive into PAN matrix causes formation of less porous structure. In addition, more regular finger-like cavities has observed in the sublayer. By increaseing SDS content, the size of finger-like cavities of sublayer has slightly changed. The effect of SDS on membrane structure can be explained as follows. The presence of SDS in polymer matix diminishes the rate of solvent exchange. Additionally, SDS molecules decreases the interaction between PAN chains due to the formation of polymer-surfactant complex. This both phenomena leads to delay demixing [25,26].

### 3.2.2. Surface properties of the prepared membranes

Fig. 5 illustrates the three dimensional AFM images for the surface of pure PAN and PAN/F-MWCNTs membranes. These images include light and dark areas that represent highest regions and valleys (or pores), respectively. Additionally roughness parameters of fabricated membranes are presented in Table 2. Two trends can be observed among surface roughness parameters with increment of F-MWCNT dosage. At first, by adding 0.5 wt.% of F-MWCNTs into polymer matrix, surface roughness of membrane reduces when compared with pure PAN membrane. This reduction is attributed to altering surface morphology and formation of smaller pores for PAN-C0.5 [27,28]. Further increasing F-MWCNTs dosage to 1 and 2 wt.% lead to the increase of the root mean roughness ($R_q$) from 4.79 nm for PAN-C0.5 to 7.31 nm for PAN-C1 and 9.64 nm for PAN-C2. It seems that, at higher dosage of F-MWCNT (>0.5 wt.%), the ionic interactions between polymer chains enhance due to presence of more amine groups on the surface of membrane. This leads to shrinking of polymer chains and subsequently rougher surfaces [27,28].

Table 2 also shows the surface CA of prepared membranes. According to the results, the highest CA has been observed for PAN0 membrane. As can be seen, the addition of F-MWCNTs and/or SDS into polymer matrix decrease CA. For PAN/F-MWCNTs mixed matrix membranes, hydrophilicity of membranes increases by increasing F-MWCNT dosage from 0.5 to 2 wt.%. This is attributed to the hydrophilic nature of F-MWCNTs owing to its hydrophilicamine group ($NH_2$) [17]. Moreover, the CA value of PAN/SDS mixed matrix membrane declines from 47.5˚ to 39.5˚ when SDS dosage increases from 0 to 5 wt.%. Indeed, hydrophilic region of SDS as anionic detergent is the reason for the reduction of CA of PAN/SDS membrane.

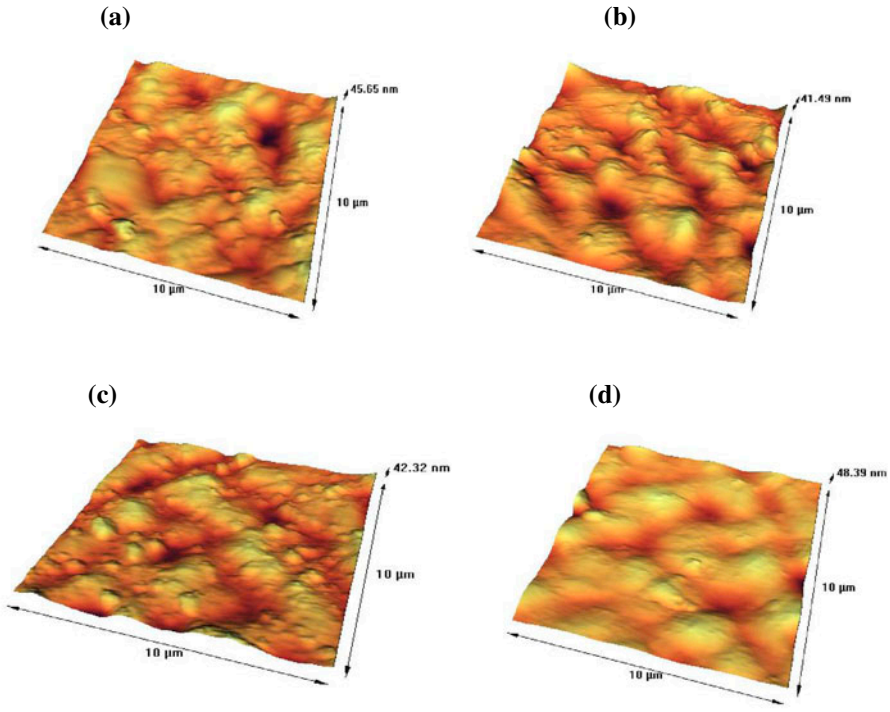


Fig. 5. AFM analysis of (a) PAN0, (b) PAN-C0.5, (c) PAN-C1, and (d) PAN-C2 membranes.

Table 2
Surface properties of the prepared membranes

| Membrane code | Contact angle (°) | $R_q$ (nm) | $R_a$ (nm) | $R_z$ (nm) |
|---|---|---|---|---|
| PAN0 | 47.5 ± 1.4 | 6.30 | 0.87 | 9.24 |
| PAN-C0.5 | 44.1 ± 1.2 | 4.79 | 0.66 | 8.36 |
| PAN-C1 | 42.4 ± 0.8 | 7.31 | 1.01 | 11.45 |
| PAN-C2 | 36.3 ± 0.9 | 9.64 | 1.34 | 12.14 |
| PAN-S2.5 | 41.0 ± 1.1 | | | |
| PAN-S5 | 39.5 ± 0.1 | | | |

### 3.3. Membrane performance

#### 3.3.1. Pure water flux

Fig. 6 shows pure water flux of prepared membranes. As illustrated, all membranes have higher pure water flux than PAN0 membrane. For PAN/F-MWCNT mixed matrix membranes, the addition of 0.5 wt.% F-MWCNT into polymer matrix increases pure water flux, considerably. The water flux improvement can be explained by surface properties and morphology of as-prepared membranes. As described before, PAN/F-MWCNTs membrane (PAN-C0.5) has more hydrophilic surface than that of the pure PAN membrane. In addition, the finger-like macrovoids have elongated across the PAN-C0.5. Besides, opened pores of F-MWCNT provide a new pathway for permeation of water molecules through PAN/F-MWCNTs membrane. On the other hand, surface of membrane become denser than that of pure PAN membrane. In this case, the effect of surface hydrophilicity of PAN-C0.5 decreases F-MWCNT influences on the top-layer structure and thus pure water flux increases [13,29–31]. By increasing F-MWCNT content, pure water flux first decreases and then increases. When concentration of F-MWCNTs increases from 0.5 to 1%, surface hydrophilicity

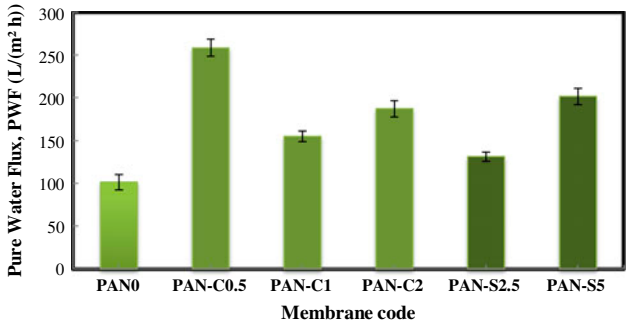


Fig. 6. Effect of MWCNTs and SDS on the pure water flux of all fabricated membranes.

increases slightly and the key influence of hydrophilicity on the enhancement of water flux of PAN-C1 reduces. As F-MWCNT dosage reaches to the 2%, CA of prepared membrane decreases from 42.4 ± 0.9 for PAN-C1 to 36.3 ± 0.9 for PAN-C2 (about 6˚). While the CA of PAN-C0.5 is 44.1 ± 1.2 (about 2˚ higher than PAN-C1). According to the results it seems that, for PAN-C2, surface hydrophilicity and new path way of water due to porous structure of F-MWCNTs are dominant factors which influence pure water flux. Anyhow, the maximum value of pure water flux is obtained at 0.5 wt.% of F-MWCNT.

In the case of PAN/SDS membrane, pure water flux increases by increment of SDS content from 0 to 5 wt.%. This trend has observed due to the change of hydrophilicity and surface morphology of PAN/SDS membranes [25]. At 2.5 wt.% of SDS dosage, membrane hydrophilicity increases while the size of macrovoids decreases. It seems that hydrophilic surface of PAN-S2.5 compensates the effect of pore size on transport rate of the water molecules through PAN-S2.5. For PAN-S5, both hydrophilicity and surface pore size of membrane are increased and as a result pure water flux is increased.

### 3.3.2. The effect of solution pH on the BSA rejection and permeate flux

The effect of the negative charge (from low to high) on the BSA rejection and permeate flux were investigated. For this objective, three pHs were selected to set the BSA solution higher than its isoelectric point (IEP, 4.8 at 25˚C) [32]. Table 3 shows BSA rejection of all as-prepared membranes in three different solution pHs. The results allow studying the effect of additives and solution pH on the rejection of BSA. As can be seen, the BSA rejection enhances when BSA solution pH increases from 5 to 9 for PAN0. The augmentation of rejection can be explained as follows. When solution pH increases, negative charge of BSA molecules enhances. Consequently, the electrostatic repulsion force between BSA and PAN0 surface increases. In this case, the transport rate of BSA molecules through the pores decreases and BSA rejection increases [33]. For PAN/F-MWCNTs membranes, the explanation of results becomes more complicated. In this case, in addition to BSA charge, rejection may be influenced by morphology and surface properties of mixed matrix membranes. When F-MWCNTs are incorporated into the polymer matrix, amine group ($NH_2^-$) on F-MWCNTs increase negative charge of membrane surface. On the other hand, BSA molecules may pass through membrane during transportation of water molecules due to high water flux of PAN-C0.5 [13,33]. This phenomenon overcomes repulsion force and as a result the BSA rejection of PAN/F-MWCNTs membranes increases when compared with the one for PAN0 membrane at the same solution pH. From Table 3, it has also observed that the BSA rejection of PAN-C0.5 decreases from 86.94 ± 2.6 to 80.30 ± 1.15% when solution pH increases from 5 to 7 due to high water flux. While, for solution pH of 9, the repulsion force prevail the high water flux of PAN-C0.5 and thus, BSA rejection increases to 93.06%. When F-MWCNT dosage is higher than 0.5% (1 and 2 wt.%), the BSA rejection becomes independent of solution pH.

As shown in Table 3, the rejection of PAN/SDS blend membranes reduces by increasing SDS concentration at the same pH value. Similar behavior was observed by Rahimpour et al. [34] who blended PES membrane by different concentration of SDS. They illustrated that the protein rejection declined at high SDS concentration due to exclusion of micelles that created membrane surface defects at higher concentration of SDS. According to the surface images of PAN/SDS membranes (Fig. 3(e)–(f)), voids are extended to the surface of PAN-S5. These voids create pass way

Table 3
BSA rejection of prepared membranes at three different pHs

| Membrane code | pH 5 | pH 7 | pH 9 |
|---|---|---|---|
| PAN0 | 82.16 ± 1.45 | 95.20 ± 1.1 | 97.26 ± 0.8 |
| PAN-C0.5 | 86.94 ± 1.6 | 80.30 ± 1.15 | 93.06 ± 1.8 |
| PAN-C1 | 94.95 ± 2.3 | 94.66 ± 0.99 | 93 ± 0.75 |
| PAN-C2 | 97.21 ± 0.13 | 97.7 ± 1.9 | 97.46 ± 1.25 |
| PAN-S2.5 | 98.1 ± 0.85 | 97.66 ± 1.01 | 98.5 ± 0.73 |
| PAN-S5 | 92.6 ± 2.3 | 93.11 ± 1.56 | 96.16 ± 1.75 |

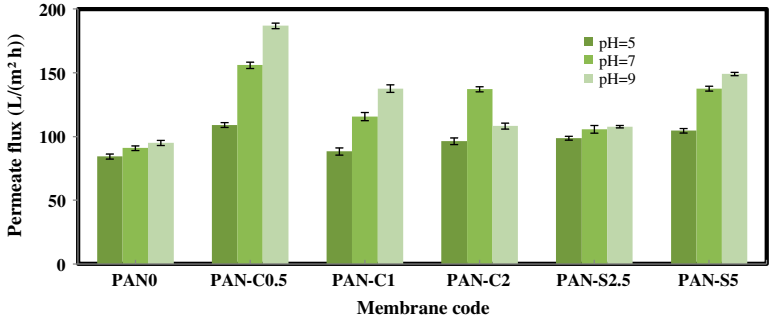


Fig. 7. Effect of MWCNTs and SDS on the permeate flux of prepared membranes at three different pHs.

for BSA molecules and decline BSA rejection of PAN-S5 when compared with PAN-S2.5. For PAN-S5, by the increment of solution pH, BSA rejection increases due to electrostatic repulsion between membrane and BSA.

Fig. 7 presents the permeate flux of pure PAN and mixed matrix membranes at different pHs. As can be seen, the permeate flux of pure PAN and PAN/F-MWCNTs membranes increase with increasing solution pH except for PAN-C2. The electrostatic repulsion between BSA molecules and membrane surface is the key motivation for increasing permeate flux. By augmenting solution pH, the repulsion force increases which prohibits adsorption of BSA molecules on the surface of membrane [33]. Beside, as reported by Vatanpour et al. [32], the hydrogen bonds is formed between hydrophilic groups (–$NH_2$/–COOH) and water molecules for PAN/F-MWCNTs membranes. This bond prevents the adsorption of protein due to formation of hydration layer and steric exclusion effect. In this case, fouling resistance decreases and consequently permeate flux increases. For PAN-C2 membrane, reduction of the permeate flux has observed with increasing the solution pH from 7 to 9. This irregular trend has been interpreted as follows. Kopac et al. [35] stated that, three dimensional structure of BSA molecule would denature at high pHs. This leads to precipitation of BSA molecules and therefore decreases permeate flux.

As can be seen in Fig. 7, permeate flux of each PAN/SDS membranes increases by increasing solution pHs. In fact, presence of the SDS molecules on the top surface of membranes negatively charged membrane surface. Furthermore, as mentioned before, negative charge of BSA molecules increases with increment of solution pH. In this case, adsorption of BSA molecules decreases, which diminishes thickness of concentration polarization layer. Accordingly, the permeate flux increases for PAN/SDS membranes by increasing solution pH [36]. Moreover, by increasing SDS dosage from 2.5 to 5%, both negative charge and pore size of membrane surface increase which enhance the permeate flux.

According to the results, one can conclude that 0.5 wt.% of F-MWCNTs and 5 wt.% of SDS are the best dosage of each additive. Beside, from Fig. 7 and Table 3, the maximum rejection and appropriate permeate flux is achieved at pH 9.0 for all as-prepared membranes.

## 4. Conclusion

To investigate the effect additives on the hydrophilicity and morphology of pure PAN membrane, SDS and F-MWCNTs were used and membranes successfully prepared by phase inversion process. FTIR analysis was conducted to assure presence of the grafted acidic (COOH) and amine ($NH_2$) surface groups onto the surface of F-MWCNTs. The proper dispersion of MWCNTs on polymer matrix was confirmed by FESEM. The as-prepared membranes were also characterized by SEM and CA analysis. SEM images showed change in pores structure by incorporating each additive. CA measurements and pure water flux showed that the addition of F-MWCNTs and SDS led to the increase in membrane hydrophilicity. The permeate flux and rejection of BSA solution increased by increasing BSA solution pH. The best results for permeate flux and BSA rejection was approximately obtained by solution pH of 9. According to the results, 0.5 wt.% of F-MWCNTs and 2.5 wt.% of SDS are the best dosages.

## References

[1] A.V.R. Reddy, D.J. Mohan, A. Bhattacharya, V.J. Shah, P.K. Ghosh, Surface modification of ultrafiltration membranes by pre-adsorption of a negatively charged polymer: I. Permeation of water soluble polymers and inorganic salt solutions and fouling resistance properties, J. Membr. Sci. 214 (2003) 211–221.

[2] L. Song, Flux decline in crossflow microfiltration and ultrafiltration: Mechanisms and modeling of membrane fouling, J. Membr. Sci. 139 (1998) 183–200.
[3] K.J. Kim, A.G. Fane, C.J.D. Fell, The performance of ultrafiltration membranes pretreated by polymers, Desalination 70 (1988) 229–249.
[4] Q. Shi, Y. Su, S. Zhu, C. Li, Y. Zhao, Z. Jiang, A facile method for synthesis of pegylated polyethersulfone and its application in fabrication of antifouling ultrafiltration membrane, J. Membr. Sci. 303 (2007) 204–212.
[5] D. Rana, T. Matsuura, Surface modifications for antifouling membranes, Chem. Rev. 110 (2010) 2448–2471.
[6] A. Asatekin, S. Kang, M. Elimelech, A.M. Mayes, Antifouling ultrafiltration membranes containing polyacrylonitrile-graft-poly(ethylene oxide) comb copolymer additives, J. Membr. Sci. 298 (2007) 136–146.
[7] H. Adib, S. Hassanajili, M.R. Sheikhi-Kouhsar, A. Salahi, T. Mohammadi, Experimental and computational investigation of polyacrylonitrile ultrafiltration membrane for industrial oily wastewater treatment, Korean J. Chem. Eng. 32 (2015) 159–167.
[8] M. Namvar-Mahboub, M. Pakizeh, Development of a novel thin film composite membrane by interfacial polymerization on polyetherimide/modified $SiO_2$ support for organic solvent nanofiltration, Sep. Purif. Technol. 119 (2013) 35–45.
[9] J. Ma, Y. Zhao, Z. Xu, C. Min, B. Zhou, Y. Li, B. Li, Role of oxygen-containing groups on MWCNTs in enhanced separation and permeability performance for PVDF hybrid ultrafiltration membranes, Desalination 320 (2013) 1–9.
[10] T. Zhou, X. Wang, H. Zhu, T. Wang, Influence of carboxylic functionalization of MWCNTs on the thermal properties of MWCNTs/DGEBA/EMI-2, 4 nanocomposites, Composites Part A: Appl. Sci. Manuf. 40 (2009) 1792–1797.
[11] N.I.M. Fadilah, A.R. Hassan, Asymmetric PVDF ultrafiltration (UF) membranes: Effect of additives & surfactants, Int. J. Chem. Environ. Eng. 5 (2014) 336–345.
[12] S.H. Zhi, R. Deng, J. Xu, L.S. Wan, Z.K. Xu, Composite membranes from polyacrylonitrile with poly(N,N-dimethylaminoethyl methacrylate)-grafted silica nanoparticles as additives, React. Funct. Polym. 86 (2015) 184–190.
[13] S. Majeed, D. Fierro, K. Buhr, J. Wind, B. Du, A. Boschetti-de-Fierro, V. Abetz, Multi-walled carbon nanotubes (MWCNTs) mixed polyacrylonitrile (PAN) ultrafiltration membranes, J. Membr. Sci. 403–404 (2012) 101–109.
[14] Y.L. Su, W. Cheng, C. Li, Z. Jiang, Preparation of antifouling ultrafiltration membranes with poly(ethylene glycol)-graft-polyacrylonitrile copolymers, J. Membr. Sci. 329 (2009) 246–252.
[15] S. Yang, Z. Liu, Preparation and characterization of polyacrylonitrile ultrafiltration membranes, J. Membr. Sci. 222 (2003) 87–98.
[16] E. Shekarian, E. Saljoughi, A. Naderi, Polyacrylonitrile (PAN)/IGEPAL blend asymmetric membranes: Preparation, morphology, and performance, J. Polym. Res. 20 (2013) 1–9.
[17] A. Amiri, M. Maghrebi, M. Baniadam, S.Z. Heris, One-pot efficient functionalization of multi-walled carbon nanotubes with diamines by microwave method, Appl. Surf. Sci. 257 (2011) 10261–10266.
[18] A. Rahimpour, M. Jahanshahi, S. Khalili, A. Mollahosseini, A. Zirepour, B. Rajaeian, Novel functionalized carbon nanotubes for improving the surface properties and performance of polyethersulfone (PES) membrane, Desalination 286 (2012) 99–107.
[19] V. Vatanpour, S.S. Madaeni, R. Moradian, S. Zinadini, B. Astinchap, Fabrication and characterization of novel antifouling nanofiltration membrane prepared from oxidized multiwalled carbon nanotube/polyethersulfone nanocomposite, J. Membr. Sci. 375 (2011) 284–294.
[20] K. Vanherck, I. Vankelecom, T. Verbiest, Improving fluxes of polyimide membranes containing gold nanoparticles by photothermal heating, J. Membr. Sci. 373 (2011) 5–13.
[21] I. Spill, A.G. Livingston, Impact of $TiO_2$ nanoparticles on morphology and performance of crosslinked polyimide organic solvent nanofiltration (OSN) membranes, J. Membr. Sci. 343 (2009) 189–198.
[22] Y. Mansourpanah, S.S. Madaeni, A. Rahimpour, Fabrication and development of interfacial polymerized thin-film composite nanofiltration membrane using different surfactants in organic phase; study of morphology and performance, J. Membr. Sci. 343 (2009) 219–228.
[23] K. Wang, M. Gu, J. Wang, C. Qin, L. Dai, Functionalized carbon nanotube/polyacrylonitrile composite nanofibers: Fabrication and properties, Polym. Adv. Technol. 23 (2012) 262–271.
[24] E. Celik, H. Park, H. Choi, Carbon nanotube blended polyethersulfone membranes for fouling control in water treatment, Water Res. 45 (2011) 274–282.
[25] N. Ghaemi, S.S. Madaeni, A. Alizadeh, P. Daraei, V. Vatanpour, M. Falsafi, Fabrication of cellulose acetate/sodium dodecyl sulfate nanofiltration membrane: Characterization and performance in rejection of pesticides, Desalination 290 (2012) 99–106.
[26] S.M. Mousavi, F. Dehghan, E. Saljoughi, S.A. Hosseini, Preparation of modified polyethersulfone membranes using variation in coagulation bath temperature and addition of hydrophilic surfactant, J. Polym. Res. 19 (2012) 1–12.
[27] M. Esmaeili, S.S. Madaeni, J. Barzin, The dependence of morphology of solid polymer electrolyte membranes on transient salt type: Effect of cation type, Polym. Int. 59 (2010) 1006–1013.
[28] K. Sears, L. Dumée, J. Schütz, M. She, C. Huynh, S. Hawkins, M. Duke, S. Gray, Recent developments in carbon nanotube membranes for water purification and gas separation, Materials 3 (2010) 127–149.
[29] S. Qiu, L. Wu, X. Pan, L. Zhang, H. Chen, C. Gao, Preparation and properties of functionalized carbon nanotube/PSF blend ultrafiltration membranes, J. Membr. Sci. 342 (2009) 165–172.
[30] H. Wu, B. Tang, P. Wu, Novel ultrafiltration membranes prepared from a multi-walled carbon nanotubes/polymer composite, J. Membr. Sci. 362 (2010) 374–383.
[31] X. Zhao, J. Ma, Z. Wang, G. Wen, J. Jiang, F. Shi, Hyperbranched-polymer functionalized multi-walled carbon nanotubes for poly (vinylidene fluoride)

membranes: From dispersion to blended fouling-control membrane, Desalination 303 (2012) 29–38.
[32] V. Vatanpour, M. Esmaeili, M.H.D. Abdi Farahani, Fouling reduction and retention increment of polyethersulfone nanofiltration membranes embedded by amine-functionalized multi-walled carbon nanotubes, J. Membr. Sci. 466 (2014) 70–81.
[33] D.A. Musale, S.S. Kulkarni, Fouling reduction in poly (acrylonitrile-co-acrylamide) ultrafiltration membranes, J. Membr. Sci. 111 (1996) 49–56.
[34] A. Rahimpour, S.S. Madaeni, Y. Mansourpanah, The effect of anionic, non-ionic and cationic surfactants on morphology and performance of polyethersulfone ultrafiltration membranes for milk concentration, J. Membr. Sci. 296 (2007) 110–121.
[35] T. Kopac, K. Bozgeyik, J. Yener, Effect of pH and temperature on the adsorption of bovine serum albumin onto titanium dioxide, Colloids Surf. A: Physicochem. Eng. Aspects 322 (2008) 19–28.
[36] N. Ghaemi, S.S. Madaeni, A. Alizadeh, P. Daraei, A.A. Zinatizadeh, F. Rahimpour, Separation of nitrophenols using cellulose acetate nanofiltration membrane: Influence of surfactant additives, Sep. Purif. Technol. 85 (2012) 147–156.